NASA TECHNICAL MEMORANDUM

NASA TM X-1710

NASA TM X-1710

EFFECT OF BLEED-SYSTEM BACK PRESSURE AND POROUS AREA ON THE PERFORMANCE OF AN AXISYMMETRIC MIXED-COMPRESSION INLET AT MACH 2.50

by Bobby W. Sanders and Robert W. Cubbison

Lewis Research Center
Cleveland, Ohio

NATIONAL AERONAUTICS AND SPACE ADMINISTRATION • WASHINGTON, D. C. • DECEMBER 1968

NASA TM X-1710

EFFECT OF BLEED-SYSTEM BACK PRESSURE AND POROUS AREA ON THE PERFORMANCE OF AN AXISYMMETRIC MIXED-COMPRESSION INLET AT MACH 2.50

By Bobby W. Sanders and Robert W. Cubbison

Lewis Research Center
Cleveland, Ohio

NATIONAL AERONAUTICS AND SPACE ADMINISTRATION

For sale by the Clearinghouse for Federal Scientific and Technical Information
Springfield, Virginia 22151 – CFSTI price $3.00

ABSTRACT

Two bleed geometries that had about a 2.75 to 1 ratio in total porous area were tested with different bleed-exit areas to provide various back pressures. With bleed-exit areas providing the same supercritical bleed mass flow, the higher porous-area configuration provided higher total-pressure recovery at critical inlet operation. For the same supercritical bleed mass flow the more porous configuration also obtained a reduction in bleed drag of 42.5 percent but at a complete loss of subcritical stability margin. However, by proper control of the bleed-exit areas, the engine corrected airflow could be decreased 13.18 percent from that at critical operation without incurring an unstart.

EFFECT OF BLEED-SYSTEM BACK PRESSURE AND POROUS AREA ON THE PERFORMANCE OF AN AXISYMMETRIC MIXED-COMPRESSION INLET AT MACH 2.50

by Bobby W. Sanders and Robert W. Cubbison

Lewis Research Center

SUMMARY

An experimental investigation was conducted to determine the effect of bleed-system back pressure and total porous area on inlet performance at Mach 2.50 in the Lewis 10- by 10-Foot Supersonic Wind Tunnel. The axisymmetric, mixed-compression inlet, with 60 percent of the supersonic-area contraction occurring internally, was designed for Mach 2.50. Boundary-layer bleed regions were located on the cowl and centerbody in both the supersonic diffuser and in the throat region. Two porous bleed configurations were tested. One had just enough porous area to remove the desired amount of bleed when choked, and the second (which had about 2.75 times the porous area of the first system) removed the desired bleed while operating unchoked. The back pressure on each of the bleed regions was varied by the utilization of a series of fixed exit areas.

For each of the two porous bleed patterns tested, the subcritical stability margin and distortion levels were degraded by reducing the bleed-exit area which reduced the bleed flow and increased the bleed recovery. With the same total bleed flow, the less porous, choked system obtained a stable margin of 7.3 percent of the engine corrected airflow, while the more porous, unchoked system had a complete loss of subcritical stable margin. However, by properly controlling the bleed-exit area of the high-porosity system, the engine corrected airflow could be decreased 13.18 percent from that at critical operation without incurring an unstart. At similar bleed flows, the more porous unchoked bleed system also provided higher bleed recoveries at an equivalent or higher inlet total-pressure recovery. The higher bleed recovery decreased the bleed drag 42.5 percent.

INTRODUCTION

A research program has been initiated at the Lewis Research Center to study the interactions between the inlet and turbojet engine of a complete propulsion system. For this purpose, an axisymmetric inlet has been designed to be used with the J-85/13 turbojet engine. This mixed-compression, shock-reflecting inlet was designed for Mach 2.5 with 60 percent of the supersonic-area contraction occurring internally. The results from a previous investigation of the effects of the amount and location of choked porous bleed on the performance of this inlet are reported in reference 1. This choked, porous bleed system provided good inlet performance and a significant stable operating range between critical operation and the unstart limit. However, this was obtained at rather low bleed pressure recovery which resulted in a drag penalty. This drag reduces airplane payload as shown in reference 2.

The present objectives were to study the effect of porous bleed area and changes in bleed back pressure on the overall inlet performance. Two porous bleed geometries having about a 2.75 to 1 ratio in total bleed area on the diffuser surfaces were tested. All bleed regions were located downstream of the oblique shock reflection points on both the cowl and centerbody. This placement of the bleed provides the best overall inlet performance as indicated in reference 1. The back pressure for each of the bleed regions was varied by using a series of fixed exit areas. A decrease in exit area results in an increase of bleed plenum back pressure and consequently an increase of bleed recovery. The variations in bleed exit area were designed such that, at one condition, the same supercritical bleed mass flow could be obtained for both bleed geometries. Bleed drag for these two configurations were calculated and compared. Similar data regarding the effect of bleed system back pressure on the performance of two similar axisymmetric mixed-compression inlets over a wider range of Mach numbers are contained in references 3 and 4.

The investigation was conducted in the Lewis 10- by 10-Foot Supersonic Wind Tunnel at zero and at maximum angle of attack before an inlet unstart. All data were obtained at a free-stream Mach number of 2.50 and a Reynolds number of 3.88×10^6 based on the cowl lip diameter.

SYMBOLS

C_D drag coefficient, based on inlet capture area

d distance from local surface, cm

h annulus height, cm

m mass flow, kg/sec

P total pressure, N/m^2

p static pressure, N/m^2

R_c cowl-lip radius, 23.66 cm

SI stability index, $SI = \left\{1 - \left[\left(W\sqrt{\theta}/\delta_{min\ S}\right)/\left(W\sqrt{\theta}/\delta\right)\right]_5\right\}100$

T total temperature, K

w weight flow rate, kg/sec

x axial distance from cone tip, cm

α angle of attack, deg

δ $P/10.131\times10^3$, N/m^2

θ T/288 K

Subscripts:

av average

b bleed

l local

max maximum

min minimum

min S minimum stable inlet operating point

P Pitot

un unstart

0 free stream

5 diffuser exit station (engine face)

APPARATUS AND PROCEDURE

Inlet Configuration

A photograph of the inlet model with cold pipe and engine mass-flow throttling plug in the Lewis 10- by 10-Foot Supersonic Wind Tunnel is shown in figure 1. This inlet was an axially-symmetric, mixed-compression configuration with 60 percent of the supersonic area contraction occurring internally. The internal compression was accomplished by a series of reflected shocks and additional isentropic compression between the reflection points. The inlet had a 12.5^o half-angle conical centerbody with a capability of translation for inlet restart. At the design free-stream Mach number of 2.50, the cap-

ture mass-flow ratio was 0.9975 (0.25 percent spillage over the cowl lip). The capture area was 0.1758 of a square meter. A complete discussion of the inlet design, including the supersonic and subsonic diffusers, is presented in reference 1. Inlet details are illustrated in figure 2. Twenty-four equally spaced vortex generators were installed on the centerbody aft of the inlet throat at station $x/R_c = 4.145$. These vortex generators (fig. 2(c)) were one-half of a NACA-0012 airfoil with the mean camber line of the airfoil as the parting line. These vortex generators had a chord length of 2.54 centimeters and a span of 1.27 centimeters. A counterrotating set of vortex generators was installed primarily to prevent centerbody flow separation during high bypass flow conditions. Ejector and overboard bypasses, indicated in figure 2(b), were sealed for this investigation.

To study the effect of bleed-system back pressure, two porous bleed patterns that are labeled M (more porous) and L (less porous) in figure 3 were designed with about a 2.75 to 1 ratio in total bleed area. All bleed regions were located downstream of the oblique shock reflection points on both the cowl and centerbody in the manner which provided the best overall inlet performance as indicated in reference 1. The back pressure for each of these bleed regions was varied by using a series of fixed exit areas. An increase in the numeric listing for configurations M and L represents a decrease in bleed-exit area and consequently an increase in bleed plenum back pressure. The bleed regions were composed of circumferential rows of holes, each 0.3175 centimeters in diameter, that were drilled normal to the local inlet surface. These holes were located on 0.4763 centimeter centers. Nominal thickness of the metal in the bleed regions was 0.3175 centimeters.

Instrumentation and Computation

Pressure instrumentation is illustrated in figure 2(b). Flow surveys were made at the entrance (station 79.63) and exit (station 93.70) of the inlet throat and at the diffuser exit (station 174.98). Overall inlet total-pressure recovery and distortion was determined by using six (10 tube) area-weighted total-pressure rakes at the diffuser exit. Bleed mass flows and recoveries were determined from measured bleed exit total and static pressures and their respective exit areas. Axial static-pressure distributions on the internal cowl and on the centerbody were also measured. Unstart angles of attack were obtained by setting an inlet operating condition and increasing the angle of attack until the inlet unstarted. The maximum unstart angle of attack was obtained by reducing the inlet pressure recovery from peak until further total-pressure recovery reduction had no effect on the unstart angle of attack.

All data were obtained at a free-stream Mach number of 2.50 and a Reynolds num-

ber of 3.88×10^6 based on the cowl-lip diameter. Data were recorded for 0° angle of attack and the maximum angle of attack before an inlet unstart.

RESULTS AND DISCUSSION

Inlet Performance

Inlet performance curves for the two porous-bleed configurations (M and L) at $\alpha = 0^\circ$ and at maximum unstart angle of attack are presented in figure 4. Data at the maximum unstart angle were not obtained for configuration L-I. Critical operation is defined as the operating condition with the terminal shock at the geometric throat. The solid symbols in figure 4 and any discussion of critical operation refer to conditions that most closely match this operation. Figures 4(a) and (c) show that the use of smaller exit areas to back pressure the bleed plenums of a given porous configuration, in general, reduced the inlet performance at critical operation, the subcritical stability margin, and the maximum unstart angle of attack. For example, about a 70-percent reduction in bleed-exit areas from configuration M-I to M-IV at $\alpha = 0^\circ$ (fig. 4(a)) decreased the inlet pressure recovery at critical operation from 0.948 to 0.924 and increased the distortion at critical operation from 0.055 to 0.105. This reduction in bleed areas for configuration M also resulted in a complete loss of subcritical stability margin and a decrease in maximum unstart angle of attack from 2.73° to 1.92°. Data that are presented in figure 4(c) for configuration L show the same trends as the data for configuration M with one exception: the critical total-pressure recovery remained about constant with increased bleed-system back pressure. Angles of attack at which the inlet unstarted are indicated in figures 4(a) and (c). Continuous operation for long periods of time was not necessarily possible at the maximum unstart angle of attack. Therefore, data that are presented in figures 4(b) and (d) are for angles of attack which are about 0.10° smaller than the maximum values indicated in figures 4(a) and (c).

The effect of decreasing bleed exit areas on the diffuser static-pressure distributions is presented in figure 5 for critical and minimum stable (minimum engine mass flow for a started inlet) operation. Pressure profiles for minimum stable operation show that the terminal shock could be positioned upstream of the geometric throat before unstart occurred. As the bleed exit areas were reduced, the distance that the terminal shock could be positioned ahead of the throat was decreased. Comparison of figures 5(b) and (d) also indicates that the forward movement of the terminal shock ahead of the throat was greater for the less porous bleed configuration L. As the terminal shock moved upstream of the geometric throat, the centerbody-pressure distributions (figs. 5(b) and (d)) were faired to indicate a separation of the boundary layer ahead of the for-

ward centerbody bleed at approximately $x/R_c = 3.22$. The fairing of these curves, which indicates the presence of the separated region, was based on a data analysis that is presented in reference 1. In reference 1 it was determined from analysis of the inlet throat and throat-exit pressure data that the separation was due to shock boundary-layer interaction. In general, this separated region did not seem to cause a decrement in overall inlet performance. A complete discussion on the extent and overall effect of this boundary-layer separation is presented in reference 1.

Bleed-System Performance

The amount of mass flow removed from the inlet through the various bleed systems at zero and at maximum unstart angle of attack is presented in figure 6 as a function of inlet pressure recovery. For constant recovery, a reduction in the bleed-exit areas of the unchoked bleed system (M) decreases the amount of bleed mass flow (figs. 6(a) and (b)). The portion of the curves that indicates a constant bleed mass flow, with varying inlet recovery, represents inlet operation with the terminal shock downstream of the bleed holes. A sharp increase in bleed flow was obtained when the terminal shock was positioned upstream of the respective bleed system. As expected, the choked bleed system flow rates were essentially insensitive to bleed exit area (figs. 6(c) and (d)).

Performance of the bleed plenums is shown in figure 7 for the same values of angle of attack. With the terminal shock downstream of the bleed regions, an exit-area decrease increased the bleed recovery and decreased the mass flow for the unchoked bleed regions of configuration M (figs. 7(a) and (b)). Data from the lowest to the maximum bleed recovery represents a forward movement of the inlet terminal shock. The maximum bleed pressure recovery data were obtained just before inlet unstart. It can be seen in figure 7(a) that the peak pressure recoveries of the various bleed regions for configuration M seem for the most part, to be limited. These limits are below the local inlet static pressure for the forward and aft cowl bleed regions. However, the bleed recovery limit for the centerbody was approximately equal to the local surface static pressure for the forward centerbody bleed. The pressure-recovery limits were about $P_b/P_0 = 0.35$ for the forward cowl bleed, $P_b/P_0 = 0.50$ for the aft cowl, and $P_b/P_0 = 0.40$ for the centerbody. These limits do not apply for the bleed on the forward cowl and centerbody of configuration M-I, which had a limit due to choking of the porous bleed regions that restricted the amount of bleed flow. For configurations L-I and L-II (fig. 7(c)) the bleed regions have choked bleed mass-flow ratio limits of about $m_b/m_0 = 0.025$ for the forward cowl, $m_b/m_0 = 0.02$ for the aft cowl, and $m_b/m_0 = 0.06$ for the centerbody. The bleed regions for configuration L-III (fig. 7(c)) seemed to be pressure recovery limited at approximately $P_b/P_0 = 0.32$ on the forward

cowl, and about 0.415 for the aft cowl and centerbody. In general, the performance of the bleed exits followed the choked orifice characteristic.

Pitot pressure profiles downstream of the forward cowl bleed and at the throat exit are shown in figure 8 for critical and minimum stable operation at zero angle of attack. For critical operation of configurations M-IV through M-I (fig. 8(a)) an increase in bleed flow provided an increased total pressure near both the cowl and centerbody. However, even though an increase in bleed was obtained in going from critical operation to the minimum stable condition (fig. 8(b)), the total pressure near the centerbody remained the same or decreased. The low total pressure for configurations M-II, M-III, and M-IV at a distance ratio $d/h = 0.08$ (station 93.70) are probably caused by bleed recirculation on the forward centerbody. An analysis of the local pressures on the centerbody surface and just inside the bleed plenum indicates that a recirculation problem could exist at minimum stable operation for these configurations. Pitot pressure profiles at critical operation for the less porous bleed pattern (L) are quite similar (fig. 8(c)). Very little change was expected because the choked bleed flows at critical inlet operation were almost identical for each of the configurations. The profiles at critical conditions for configuration L are also similar to the pressure profile of configuration M-IV (fig. 8(a)), which had about the same total bleed mass-flow ratio. The dip in the throat exit rake profile for minimum stable conditions (fig. 8(d)) at a distance ratio $d/h = 0.64$ was caused by an altered inlet shock system that was the result of the separated boundary layer (fig. 5(d)) on the forward centerbody. This separation did not seem to affect the recovery near the centerbody as shown in figure 8(d). An analysis of the local pressures on the centerbody surface and in the bleed plenum indicates that the forward centerbody bleed flow does not recirculate for configuration L.

Bleed Drag Comparison

A comparison of inlet performance of two configurations having the same supercritical bleed flow is shown in figure 9. One configuration (L-I) was a low porosity, low bleed-recovery system with the bleed holes choked. The other (M-IV) was a high-porosity configuration with the bleed exits controlling the bleed flow (unchoked porous surface). The high-porosity configuration provided higher total-pressure recovery at critical inlet operation at approximately the same bleed mass flow. However, the subcritical stable margin was reduced from 7.3 percent of the engine corrected airflow to a complete absence of subcritical stability. At similar bleed flows, the more porous system has higher bleed recoveries with the equivalent or higher inlet recovery. Therefore, from a bleed drag viewpoint it is probably desirable to use configuration M-IV. However, to reduce the possibility of an inlet unstart the stable range must be increased unless

supercritical operation is acceptable. To avoid the performance penalty associated with supercritical inlet operation, it would be desirable to provide proper control of bleed exit area. Figure 9 indicates the inlet performance that may be expected from configuration M-IV by this procedure. It was obtained from the data of figure 4(a) by fairing a curve through the critical points for the various exit areas of configurations M-IV to M-I. In an actual application, control of this bleed area variation would be required to either anticipate disturbances that might cause an unstart or else to actuate so rapidly that an unstart is averted. The resulting range of stability shown in figure 9 is equivalent to a 13.18-percent decrease in engine corrected airflow from that at critical operation of configuration M-IV. Most of this range (10.55-percent corrected airflow) resulted from increased bleed with the shock remaining at the critical position. In effect, then, the increased bleed area was equivalent in concept to a throat bypass. The remaining part of the stability range resulted from the subcritical stability of the wide open bleed-exit configuration (M-I). For reference purposes the performance of the low porosity configuration that provided the most stable range (L-I) is also shown in figure 9.

In reference 2 the variation of bleed drag coefficients with bleed mass flow for various bleed recoveries were calculated by assuming a sonic axial discharge. These data are presented in figure 10. Data that represent total bleed flow for an inlet-engine match at an inlet mass-flow ratio of $m_5/m_0 = 0.947$ for configurations M-IV and L-I are presented in figure 10. A mass weighted total-pressure recovery for the three bleed regions was calculated for these data points. It is apparent that back pressuring the high-porosity configuration (M-IV) to maintain the same amount of bleed flow as a low porosity configuration (L-I) provided a significant reduction in bleed drag. Comparison of the data in figure 10 indicates a 42.5-percent reduction in drag coefficient (0.056 to 0.0322).

Effect of Bleed System Back Pressure and Porous Area on Payload Capability of Typical Supersonic Aircraft

For supersonic cruise applications, it is desirable to operate at the maximum payload condition. However, it is also desirable to have sufficient stability margin to minimize the possibility of an inlet unstart due to a sudden throttle decrease or afterburner hard light. Disturbances such as these are typically on the order of 7 percent in engine corrected airflow. To assess the penalty involved in operating the bleed configurations (M and L) over a range of stability margins, the change in payload resulting from a trade-off between bleed mass-flow rate and inlet recovery was calculated. This payload change in terms of passengers was calculated using the results of an unpublished Mach 2.7 supersonic transport mission study similar to that reported in reference 2 for a

Mach 3 aircraft. This analysis assumed a 208-passenger aircraft with a total range of 6480 kilometers. These results indicate that a 0.01 change in recovery and bleed drag coefficient produces a passenger change of 4.05 and 4.75, respectively. The reference point (zero increment in passengers) was assumed to be at 90-percent pressure recovery with a bleed drag coefficient of 0.035. Pressure recovery data that are presented in figure 4 were used to determine the effect of inlet-recovery variation. The respective bleed drag coefficients were calculated from the bleed data that are presented in figure 7 assuming a sonic axial discharge. The payload penalties in terms of passengers for configurations M and L for various stability indices and distortion levels are presented in figure 11. Stability index SI is defined as the percentage change in engine corrected airflow between any given operating condition and the minimum stable condition. In general, increasing the bleed back pressure (increase in configuration numeric listing) increased the payload capability for stability indices below 5 percent. However, this was obtained at an increase in distortion level. At a stability index of 7 percent the configurations with moderate bleed back pressures (M-II and L-II) appear to be somewhat better than the configurations with higher back pressure. Previously, it was shown (fig. 9) that combining the performance characteristics of configuration M-IV with variable bleed-exit areas would provide a significant stable operating margin and maintain a high bleed-system performance level. This proposed configuration is compared in figure 12 with the original configuration (M-IV) and with one of the less porous configurations (L-I), which had the same supercritical bleed mass flow. At a stability index of 7 percent it is apparent that the required reduction in inlet-pressure recovery for configuration M-IV (fixed bleed exits) offset the reduced drag that was obtained by bleed back pressuring. Consequently, to obtain a stability index of 7 percent with fixed bleed-exit systems, the less porous bleed configuration (L-I) was more efficient. With variable bleed-exit areas, it would be possible to achieve the sizeable gains indicated for configuration M-IV in figure 12. As a result, it would be possible to take advantage of both the high pressure recovery and the reduction of bleed drag (high bleed recovery) and actually provide a stability index of about 13.18 percent (almost double the proposed required amount). Simultaneously, the payload would be increased by 10 passengers above zero change in number of passengers for a typical mission of a supersonic aircraft.

SUMMARY OF RESULTS

A wind tunnel investigation has been conducted to determine the effect of back pressuring the bleed systems of a high-performance, mixed-compression inlet designed for Mach 2.50. Two porous bleed patterns, one containing 2.75 times the porous area of the

other, were back pressured by utilizing various fixed-bleed-exit areas. The high-porosity, high-bleed recovery configuration was designed to operate with the bleed holes unchoked. One of the unchoked configurations was designed to maintain the same amount of supercritical bleed flow as a less-porous, choked, low-bleed recovery configuration. The following results were obtained:

1. Bleed mass flow was reduced by increasing the back pressure for a given porous bleed configuration. This reduction in bleed flow for a given configuration caused a decrease in overall inlet performance.

2. A high-porosity bleed system that was back pressured to obtain the same supercritical bleed flow as a less porous, choked, low bleed-recovery configuration obtained a higher total-pressure recovery at critical inlet operation.

3. A complete loss of subcritical stability resulted from back pressuring the high-porosity configuration to maintain the same supercritical bleed as a less porous system. However, by proper control of the bleed exit areas of the high-porosity system, the engine corrected airflow could be decreased 13.18 percent from that at critical operation without incurring an unstart. Simultaneously, the payload would be increased by 10 passengers above zero change in number of passengers for a typical mission of a supersonic aircraft.

4. Proper back pressuring of a high-porosity bleed system to maintain the same amount of bleed flow as a low-porosity, choked, low bleed-recovery configuration can reduce the bleed drag by 42.5 percent at similar inlet performance.

Lewis Research Center,
National Aeronautics and Space Administration,
Cleveland, Ohio, August 9, 1968,
126-15-02-11-22.

REFERENCES

1. Cubbison, Robert W.; Meleason, Edward T.; and Johnson, David F.: Effect of Porous Bleed in a High-Performance, Axisymmetric, Mixed-Compression Inlet at Mach 2.50. NASA TM X-1692, 1968.

2. Koenig, Robert W.: Inlet Sensitivity Study for a Supersonic Transport. NASA TN D-3881, 1967.

3. Sorensen, Norman E.; and Smeltzer, Donald B.: Investigation of a Large-Scale Mixed-Compression Axisymmetric Inlet System Capable of High Performance at Mach Numbers 0.6 to 3.0. NASA TM X-1507, 1968.

4. Smeltzer, Donald B.; and Sorenson, Norman E.: Investigation of a Nearly Isentropic Mixed-Compression Axisymmetric Inlet System at Mach Numbers 0.6 to 3.2. NASA TN D-4557, 1968.

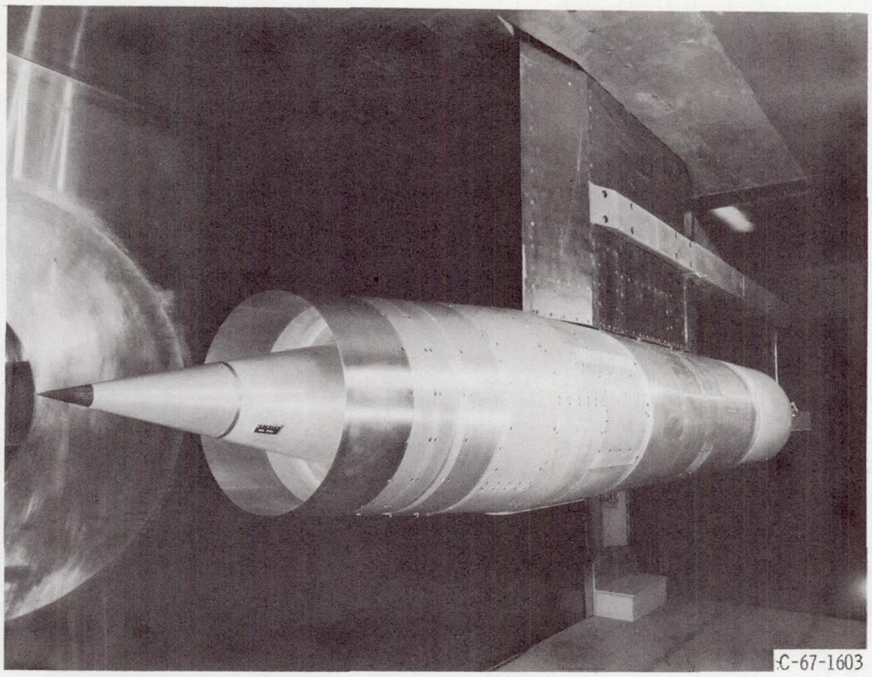

Figure 1. - Model installed in 10- by 10-foot Supersonic Wind Tunnel.

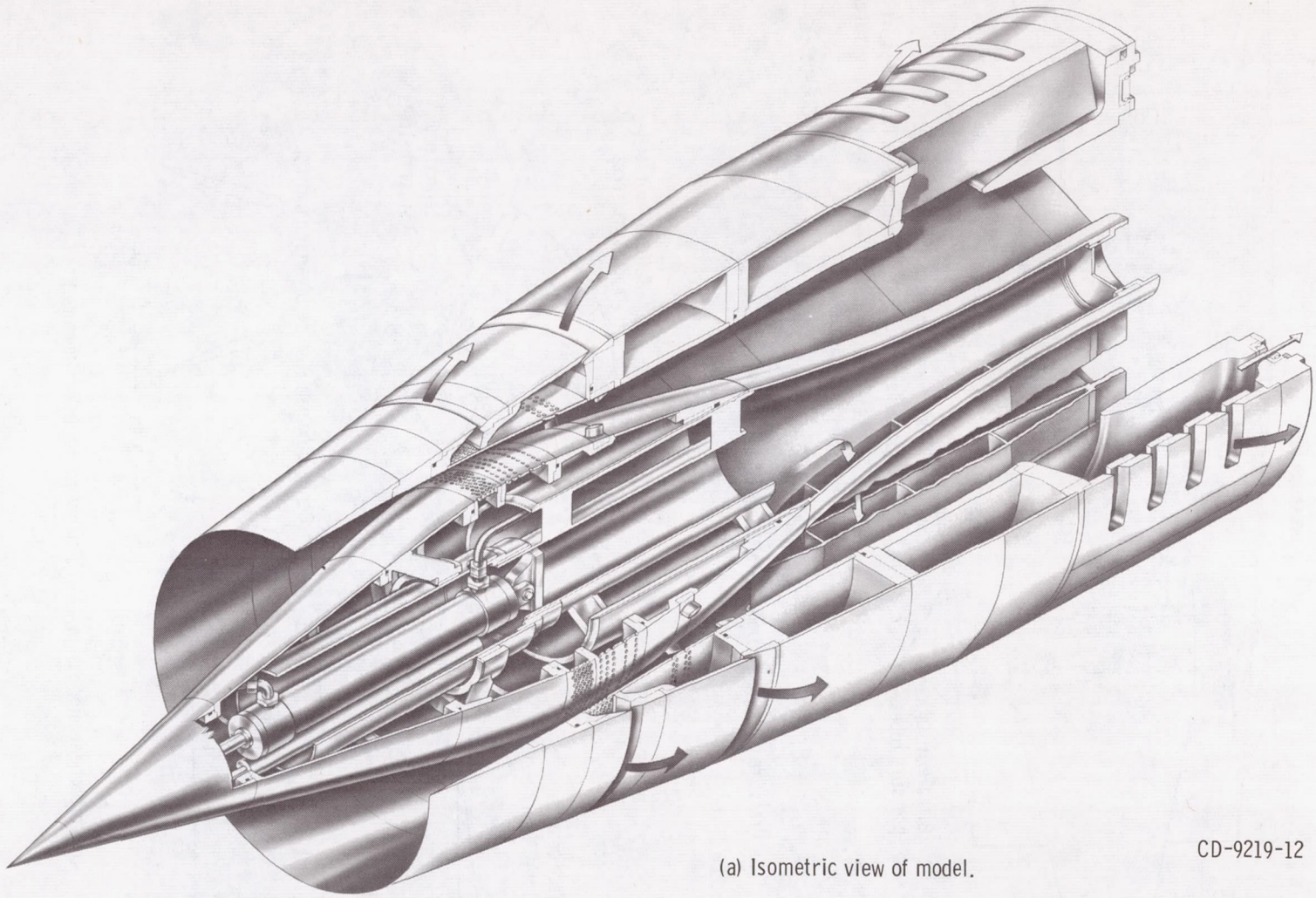

(a) Isometric view of model.

CD-9219-12

Figure 2. - Model details.

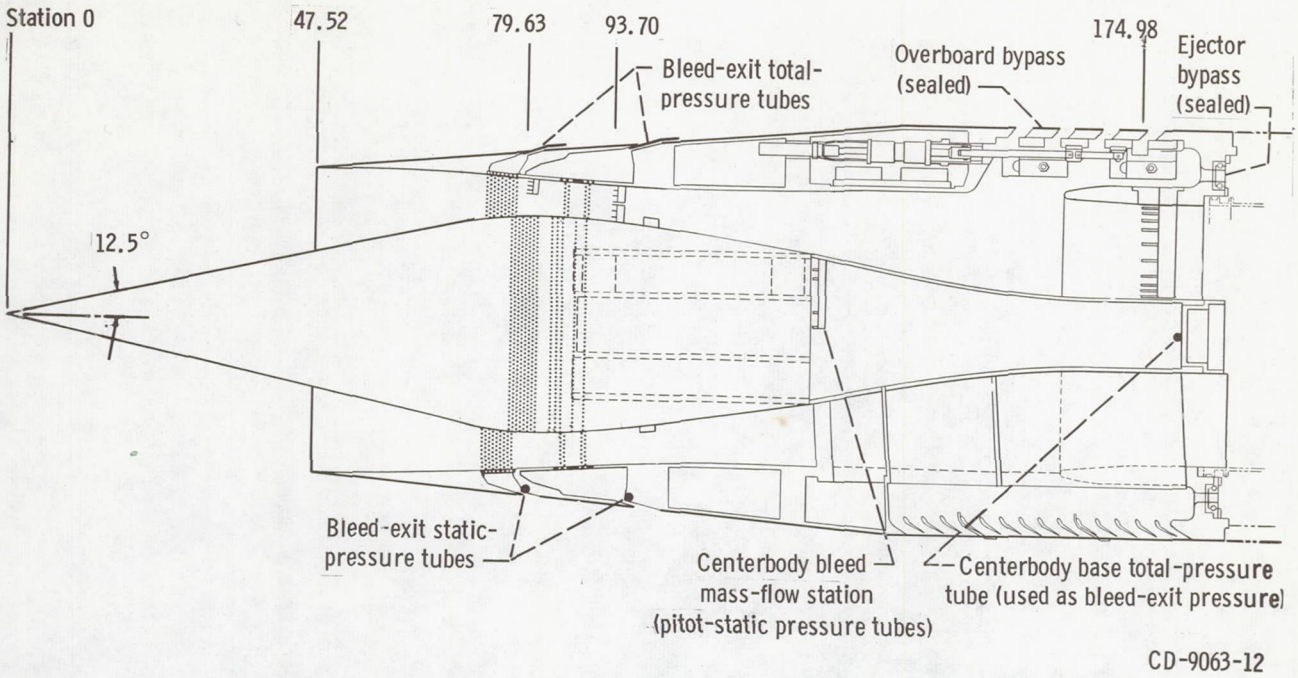

(b) Pressure instrumentation. (Station numbers are in centimeters.)

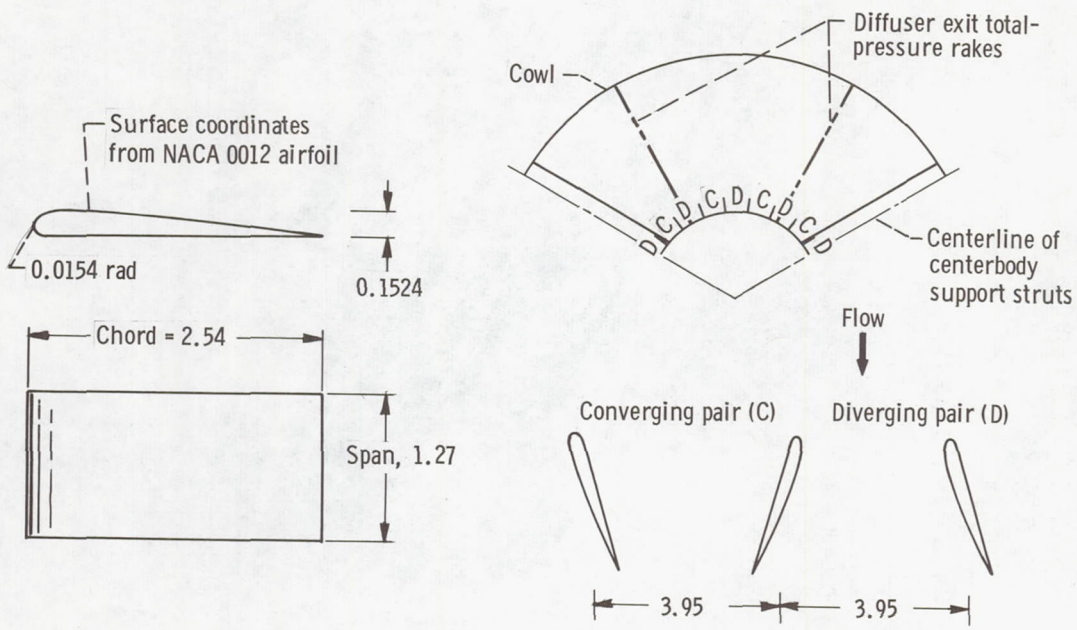

(c) Vortex generator design. (All dimensions are in centimeters.)

Figure 2. - Concluded.

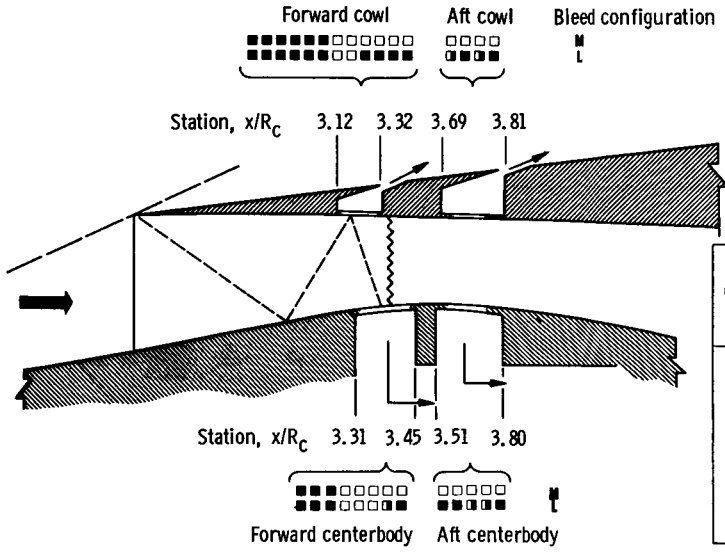

Bleed configuration	Forward cowl	Aft cowl	Centerbody
	Bleed-exit area, cm^2		
M-I	110.4	84.2	212.6
M-II	73.4	49.7	129.9
M-III	55.0	34.4	106.3
M-IV	30.9	20.6	67.0
L-I	110.4	84.2	212.6
L-II	73.4	49.7	129.9
L-III	46.5	20.6	67.0

Figure 3. - Bleed-inlet configurations. Total porous area for bleed configuration M, 409.6 square centimeters; for bleed configuration L, 149.5 square centimeters.

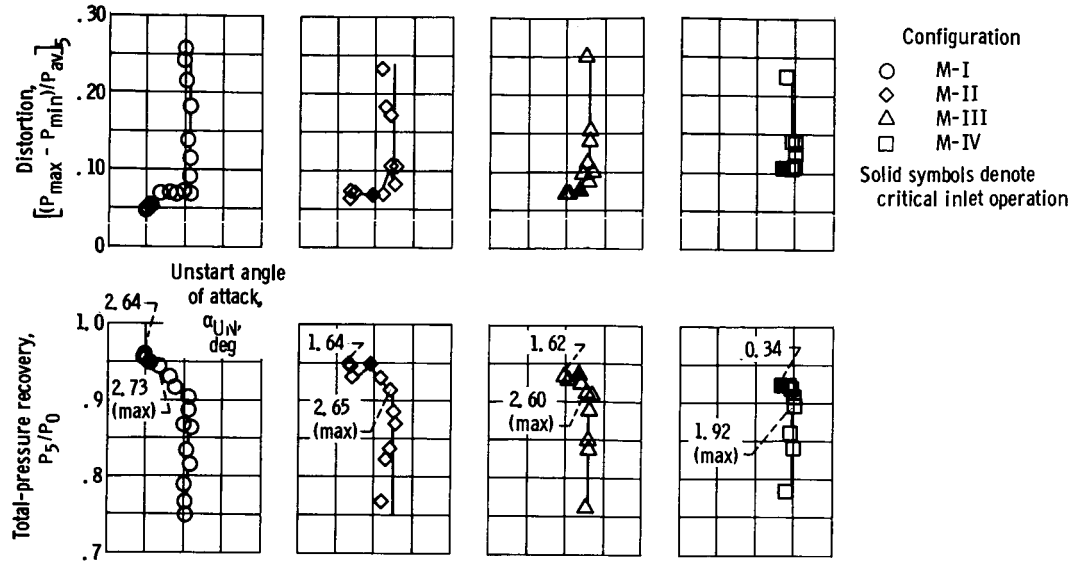

(a) Configuration M; angle of attack, zero.

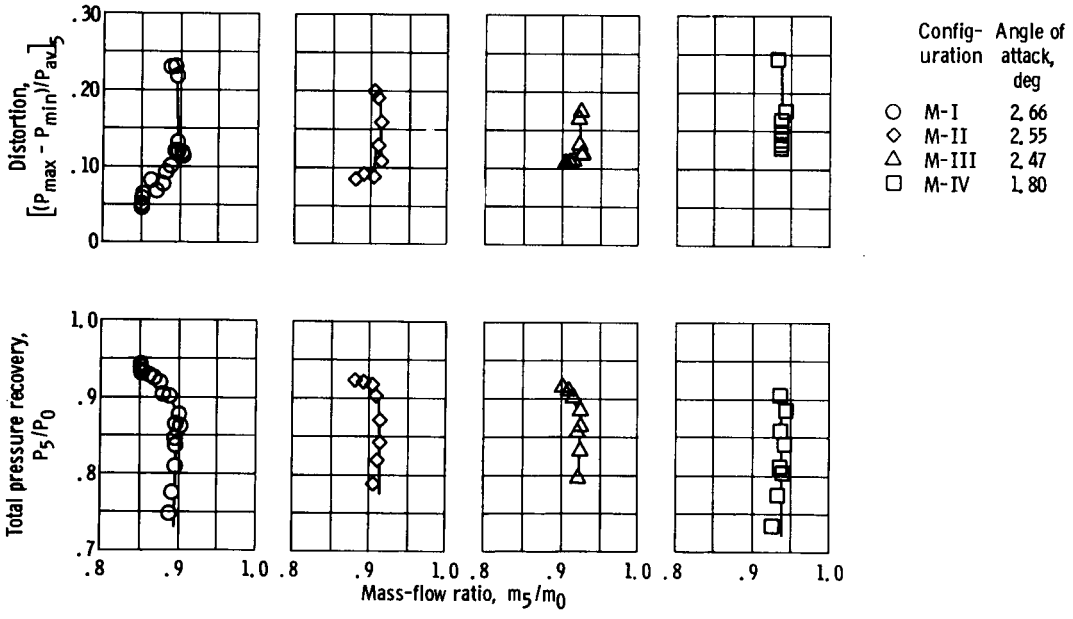

(b) Configuration M; angle of attack, maximum unstart angle.

Figure 4. - Effect of varying bleed-exit areas on inlet performance at Mach 2.50.

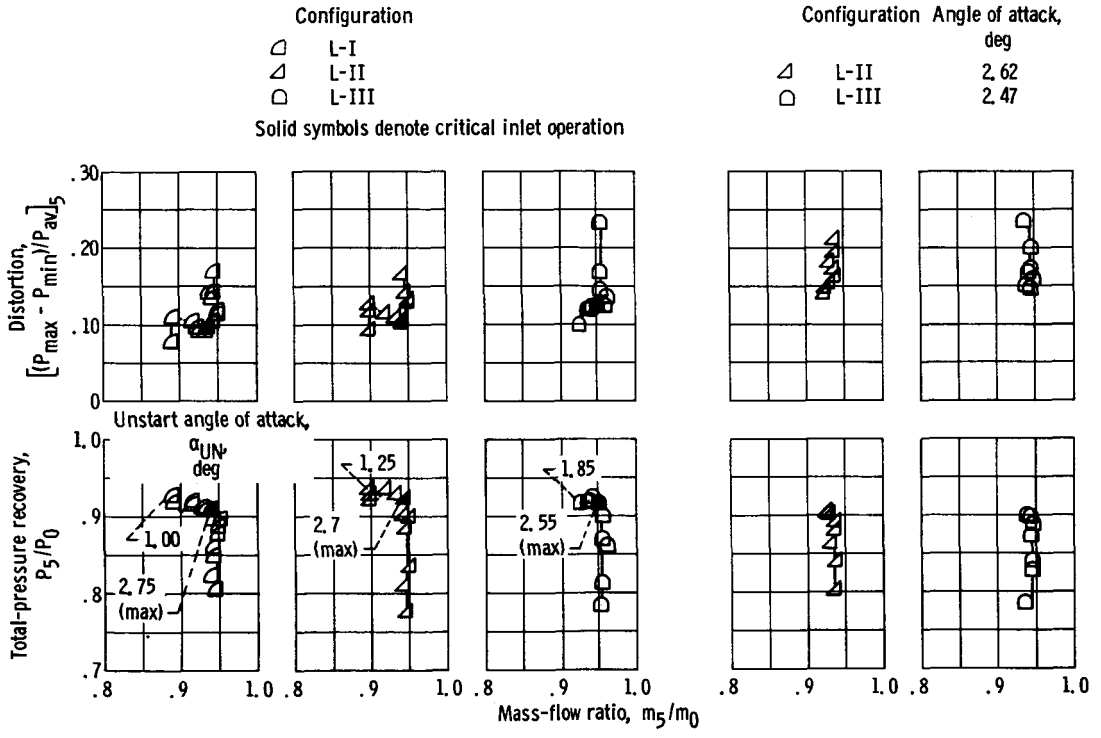

(c) Configuration L; angle of attack, zero.

(d) Configuration L; angle of attack, maximum unstart angle.

Figure 4. - Concluded.

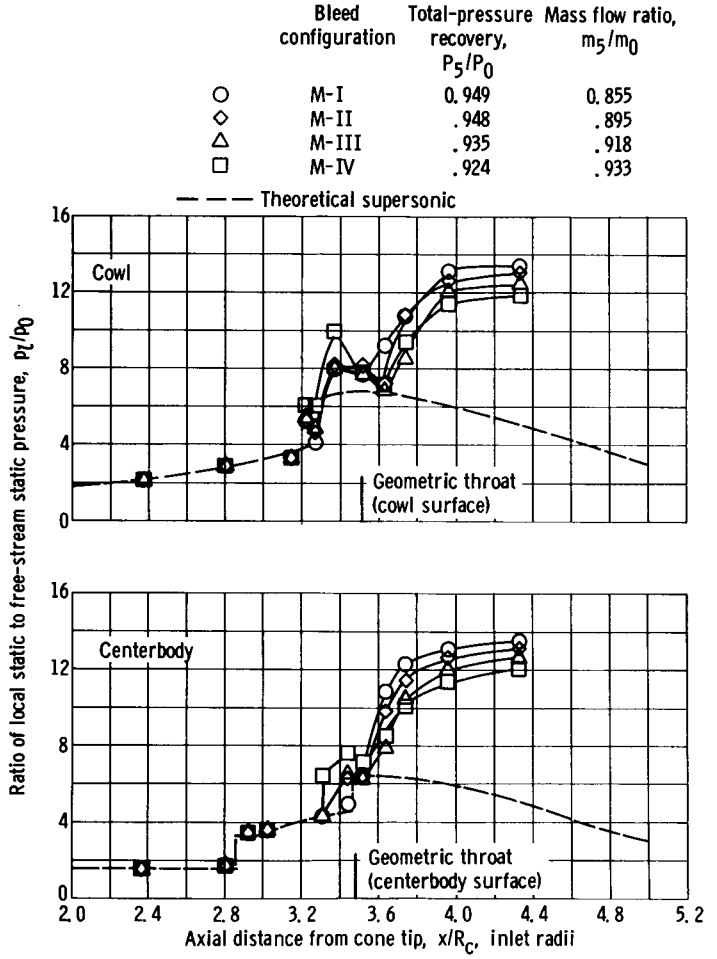

(a) Critical inlet operation for configuration M.

Figure 5. - Effect of back pressuring bleed systems on diffuser static-pressure distributions. Mach number, 2.50; angle of attack, zero.

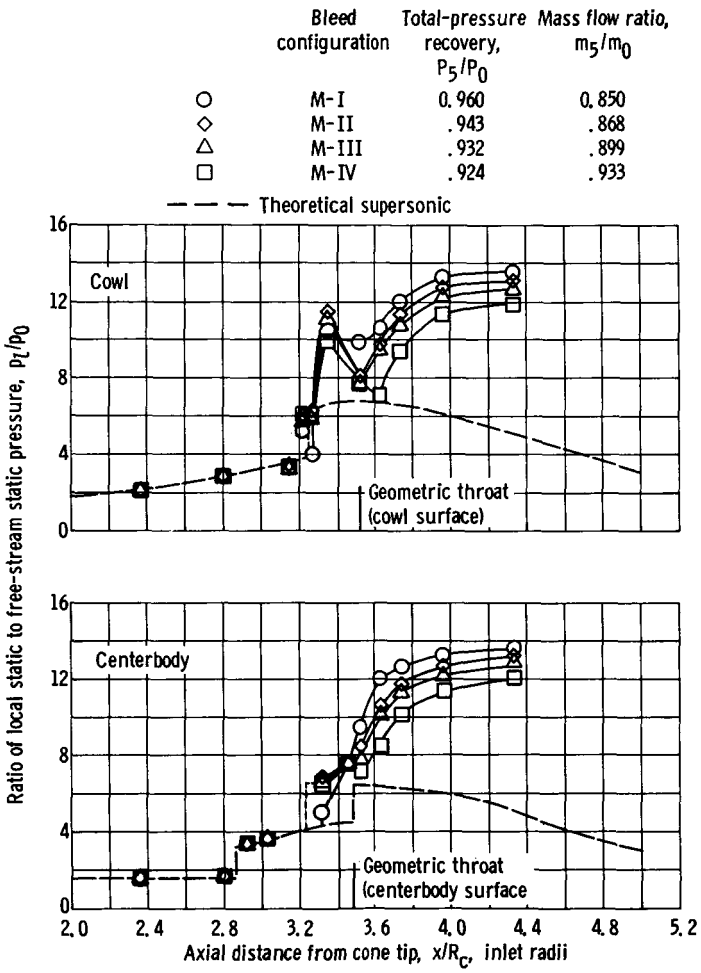

(b) Minimum stable inlet operation for configuration M.

Figure 5. - Continued.

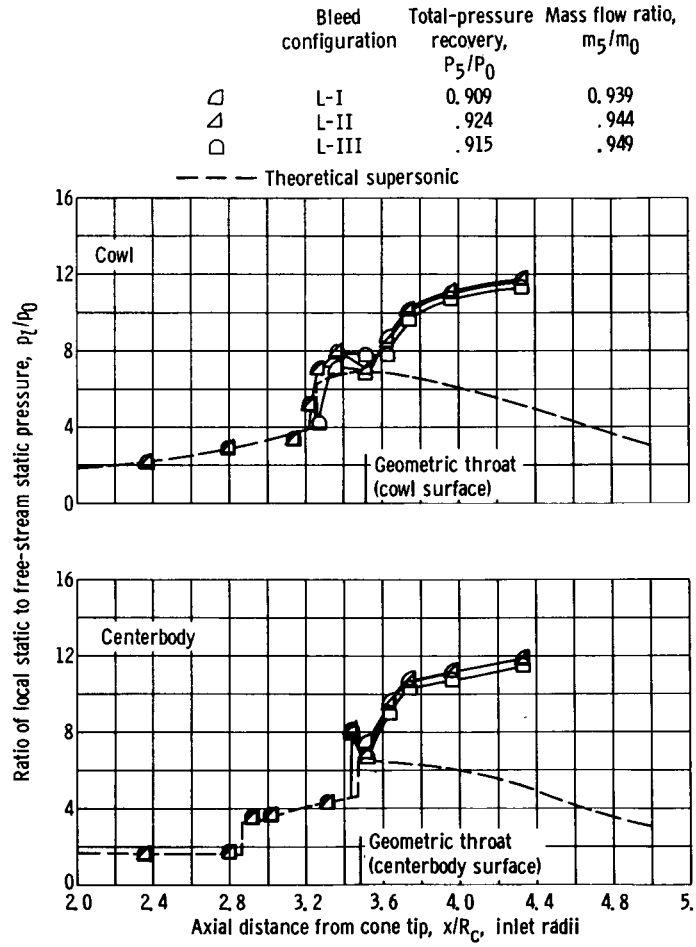

(c) Critical inlet operation for configuration L.

Figure 5. - Continued.

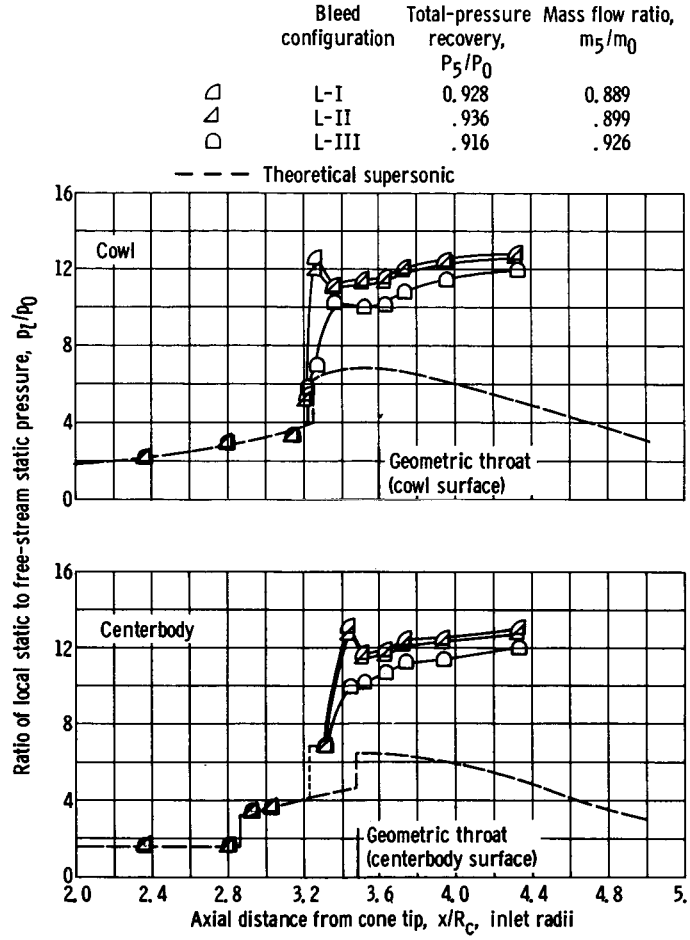

(d) Minimum stable inlet operation for configuration L.

Figure 5. - Concluded.

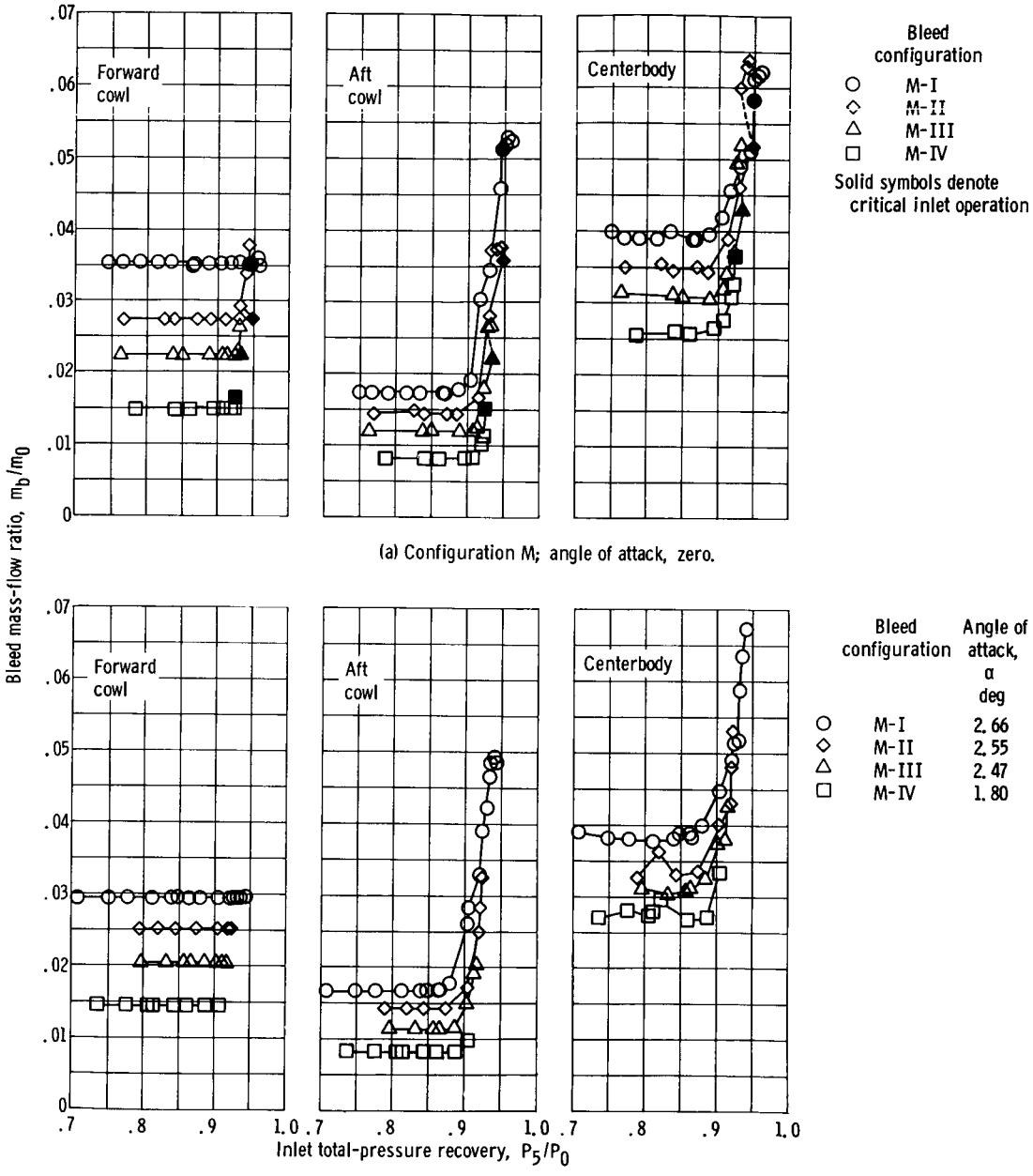

(a) Configuration M; angle of attack, zero.

(b) Configuration M; angle of attack, maximum unstart angle.

Figure 6. - Variation of bleed mass-flow ratio with inlet recovery at Mach 2.50.

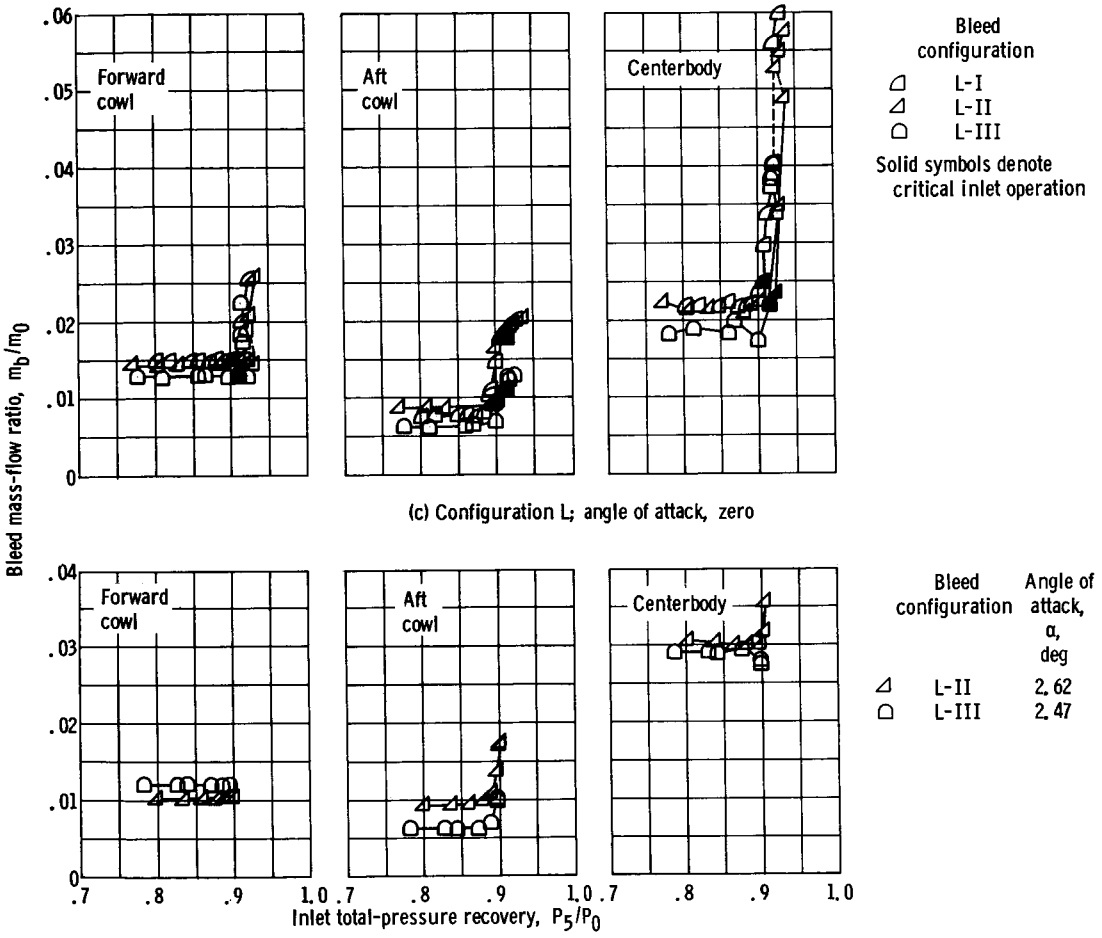

(c) Configuration L; angle of attack, zero

(d) Configuration L; angle of attack, maximum unstart angle.

Figure 6. - Concluded.

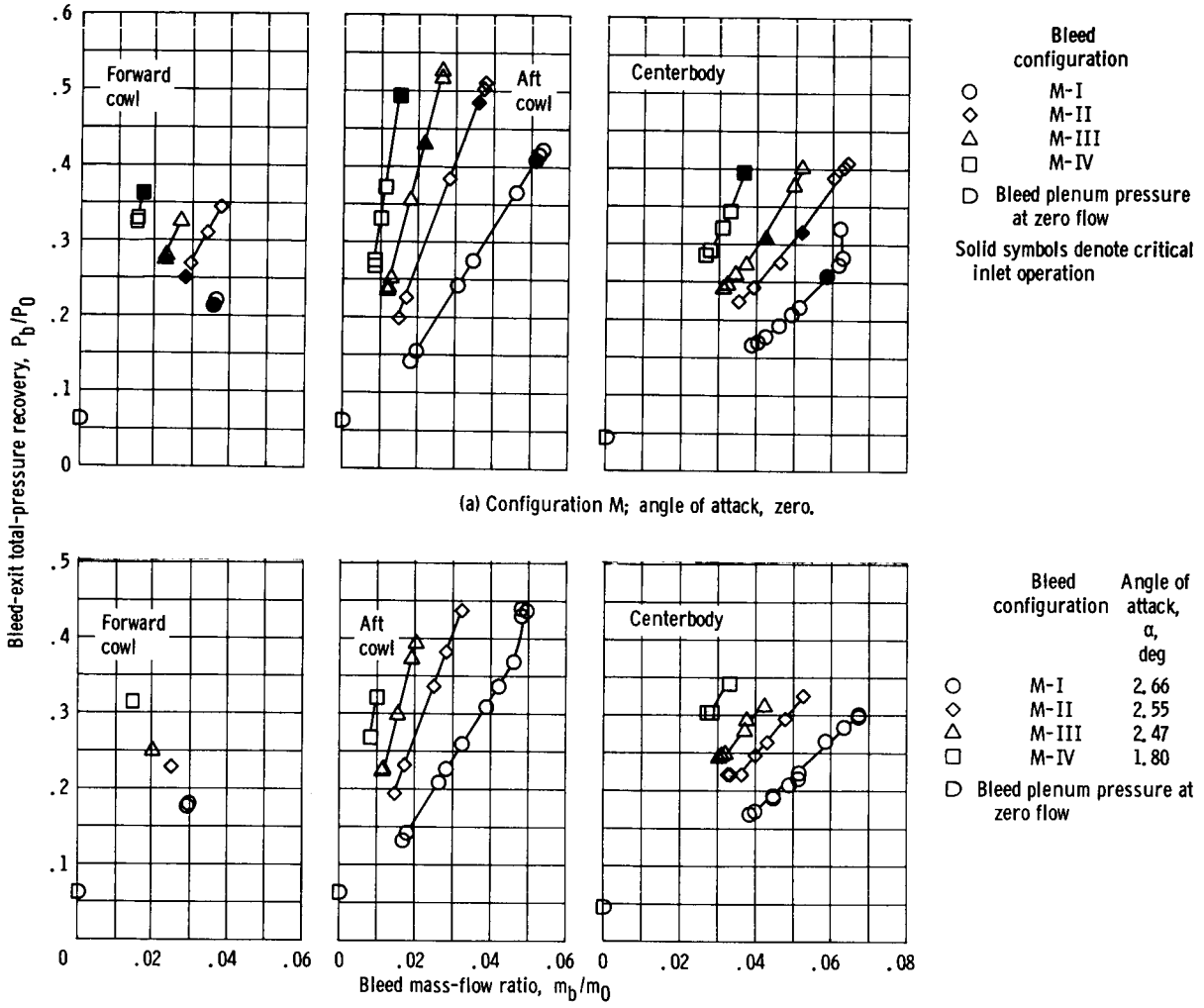

(a) Configuration M; angle of attack, zero.

(b) Configuration M; angle of attack, maximum unstart angle.

Figure 7. - Bleed plenum performance for constant bleed-exit areas at Mach 2.50.

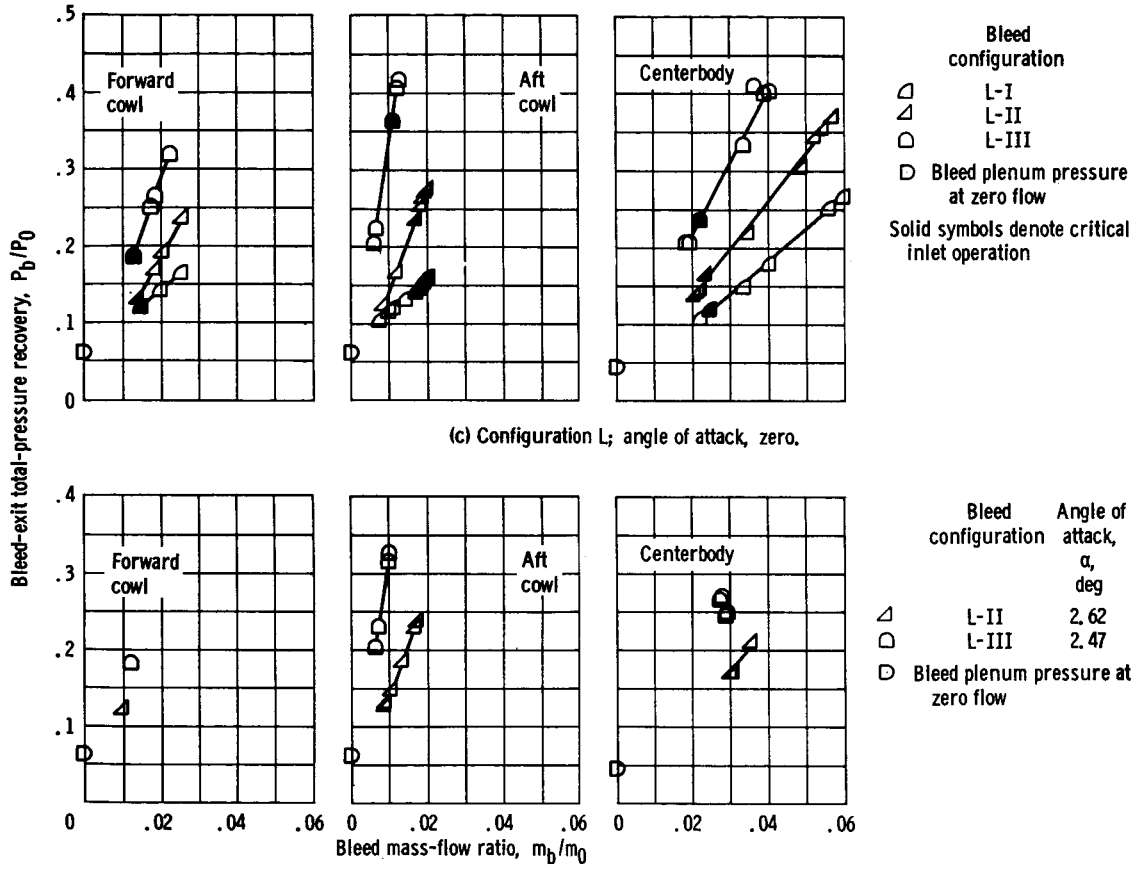

(c) Configuration L; angle of attack, zero.

(d) Configuration L; angle of attack, maximum unstart angle.

Figure 7. - Concluded.

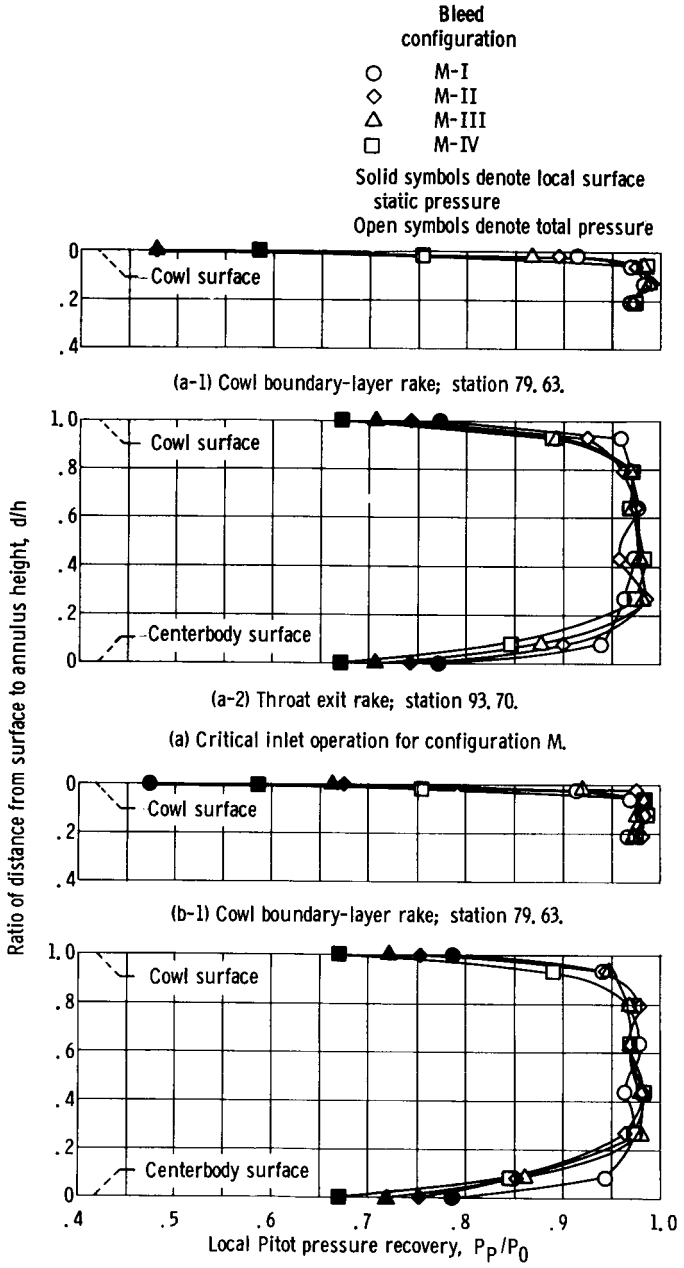

(a-1) Cowl boundary-layer rake; station 79.63.

(a-2) Throat exit rake; station 93.70.

(a) Critical inlet operation for configuration M.

(b-1) Cowl boundary-layer rake; station 79.63.

(b-2) Throat-exit rake; station 93.70.

(b) Minimum stable inlet operation for configuration M.

Figure 8. - Effect of back pressuring bleed systems on inlet throat flow conditions: Mach number, 2.50; angle of attack, zero.

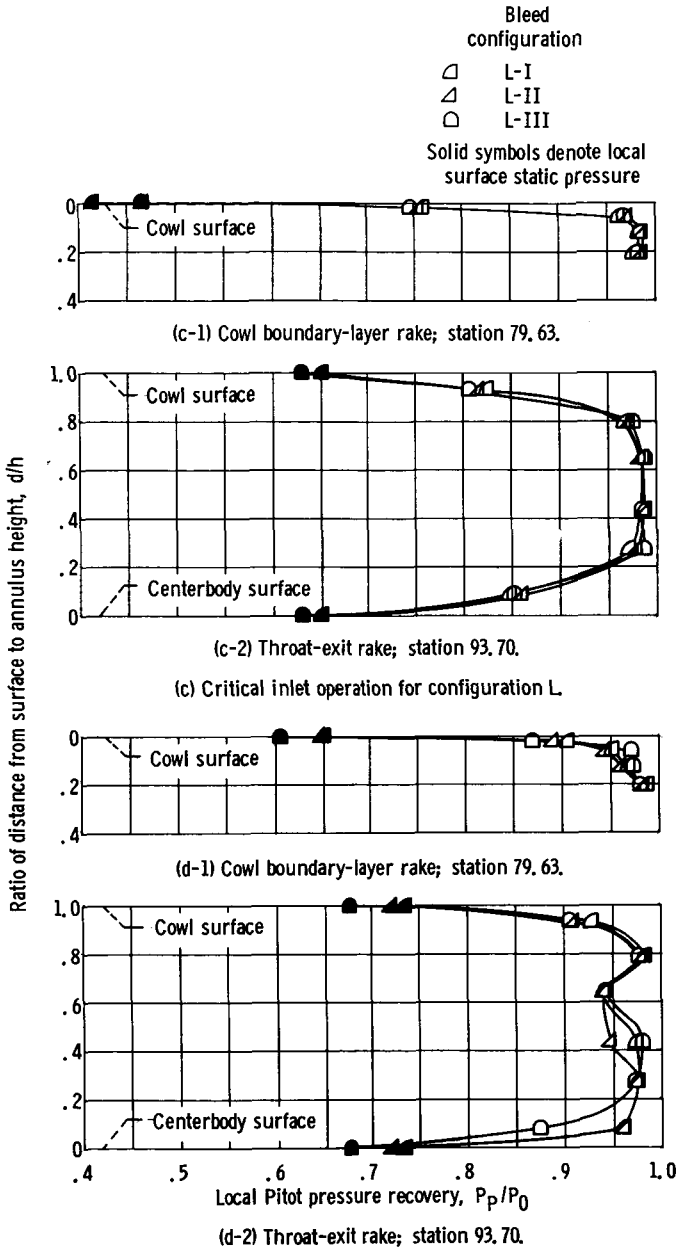

(c-1) Cowl boundary-layer rake; station 79.63.

(c-2) Throat-exit rake; station 93.70.

(c) Critical inlet operation for configuration L.

(d-1) Cowl boundary-layer rake; station 79.63.

(d-2) Throat-exit rake; station 93.70.

(d) Minimum stable inlet operation for configuration L.

Figure 8. - Concluded.

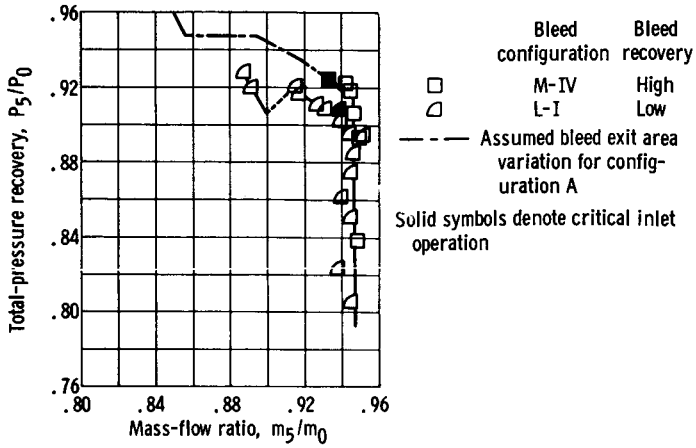

Figure 9. - Comparison of inlet performance for low-porosity, low-recovery bleed configuration with high-porosity bleed configuration utilizing assumed bleed exit area variation. Mach number, 2.498; angle of attack, zero.

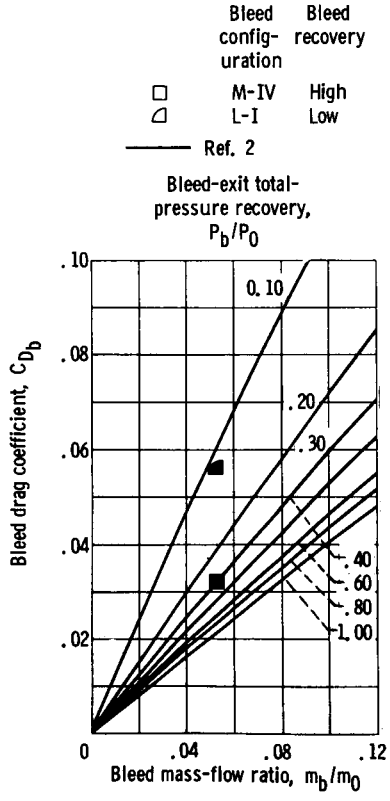

Figure 10. - Comparison of bleed drag between low and high recovery bleed systems at inlet-engine match condition. Mach number, 2.50; angle of attack, zero. (Data points represent engine match condition at supersonic cruise with $m_5/m_0 = 0.947$.

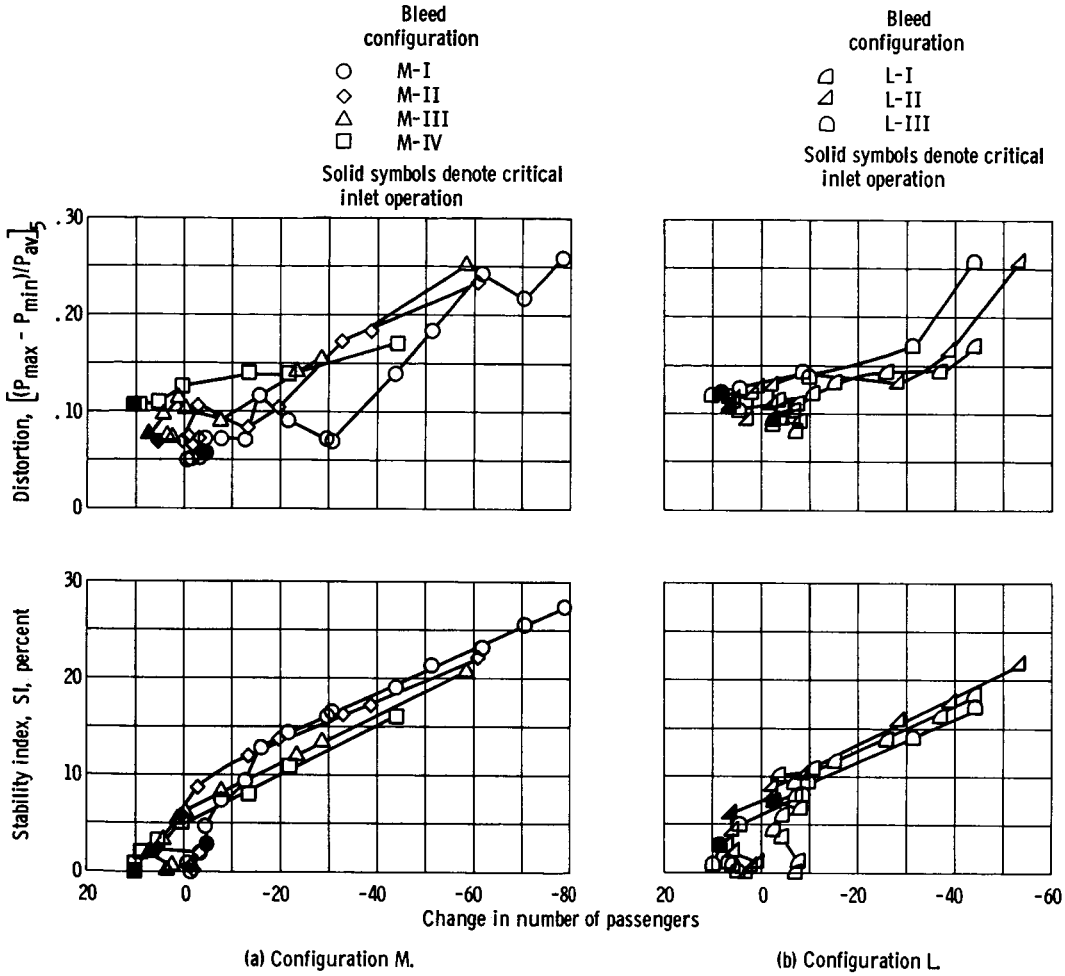

Figure 11. - Effect of bleed back-pressuring on inlet stability and distortion with change in number of passengers for typical mission of supersonic aircraft. Mach number, 2.50; angle of attack, zero.

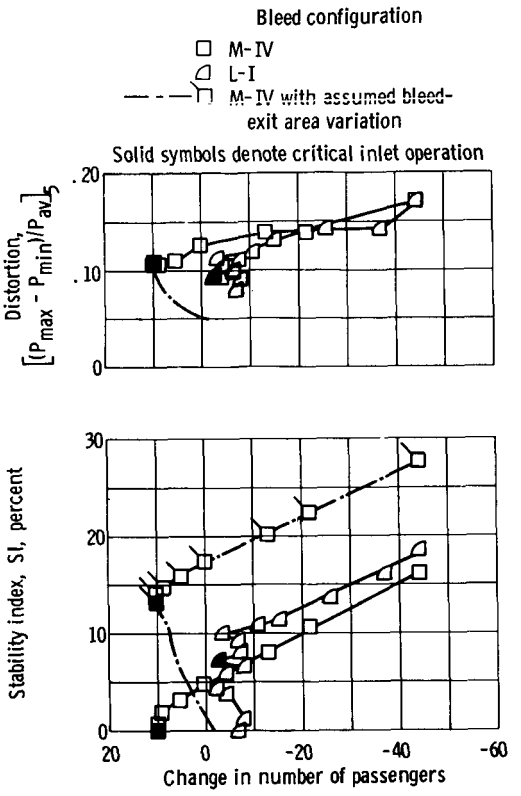

Figure 12. - Comparison of stability and distortion with decrement in passengers for low- and high-porosity bleed system that has fixed exit areas and high-porosity utilizing an assumed bleed-exit area variation for typical mission of supersonic aircraft. Mach number, 2.50.

NASA-Langley, 1968 — 1 E-4604